ASSESSMENT OF HYDROGEN FUEL TANK INTEGRATION AT AIRCRAFT LEVEL

D. Silberhorn, G. Atanasov, J-N. Walther, T. Zill
German Aerospace Center (DLR), Institute of System Architectures in Aeronautics,
Hein-Saß-Weg 22, 21129 Hamburg, Germany

Abstract

The assessment of different hydrogen tank concepts and shapes at aircraft level for a typical short/mid-range aircraft with an entry into service of 2045 is the main focus of this paper. Hydrogen is one potential option to store energy inside an air vehicle. The low gravimetric density together with the cryogenic characteristic of liquid hydrogen result in tank shapes which are challenging to integrate into an aircraft. For this integration, a multidisciplinary design approach is employed in which the effects on aircraft level of the most relevant aspects of the tank design are taken into account. This includes a mid-fidelity thermal tank representation to model its thermal behavior and to capture the relevant sensitivities. This model together with the fuel containment and fuel system mass methodology is implemented into the overall aircraft design environment. Additionally, the effects of the tank integration on the airframe structure and the aerodynamic behavior together with safety and operational aspects and an in-flight trim drag calculation are considered.
The main trade-off for the investigated aircraft concepts is between the liquid-hydrogen tank boil-off and the insulation mass effect coupled with different tank geometries on mission fuel consumption. Furthermore, the matter of engine and aerodynamic performance matching, which is highly different for hydrogen fueled aircraft, is studied.
To ensure a fair comparison, a sophisticated investigation for several baseline aircraft at the timeframe of 2045 is conducted which represent the best possible conventional aircraft, i.e. a kerosene fueled aircraft with a high aspect ratio wing, increased engine efficiency and structural mass reduction.
Besides the discussion of the performance characteristics for a short/mid-range aircraft class fueled with hydrogen for selected tank positions, the driving phenomena are described and assessed.

Keywords

Overall Aircraft Design; Hydrogen fueled Aircraft; Conceptual Liquid Hydrogen Tank Design; Technology Integration; Technology Assessment

1. INTRODUCTION

The share of the total climate-damaging emissions of aviation will increase in the upcoming decades due to the massive global growth on the one hand and because of the reduced impact of other transportation sectors. This represents a risk to the aviation industry which causes together with the challenging goals set up by the Flightpath 2050 [1] the need to investigate new concepts and ideas. One potential solution is to use hydrogen as the main energy source which can either be burned in a gas-turbine, converted to electrical energy via a fuel-cell or a combination of both. Assuming a challenge between synthetic kerosene produced by power to liquid (PtL) procedures and hydrogen in the future for short, mid and long-range aircraft, hydrogen has the advantage of more energy efficient production compared to PtL kerosene assuming electric energy as the power source and water and CO2 captured from the air as the main resources. Nevertheless, using hydrogen as fuel comes also with several challenges considering the infrastructure and the storage inside an aircraft which is why the latter one is content of the following study.
Hydrogen has approximately 2.8 times less mass per amount of energy but also 4 times more volume in a liquid state [2]. Storing the hydrogen at a pressure of 164bar and a temperature of 288.15K, would result in 5.6 times as much volume as kerosene for the same amount of energy, which can be competitive with the liquid form of storage hydrogen [3]. Nevertheless, despite several advantages of pressurized gaseous hydrogen storage, the mass of highly pressurized tanks would exceed the limit of feasibility for commercial aircraft. Hence, storing hydrogen at its liquid state at approximately -253°C has been chosen to be preferable. The huge volume together with the cryogenic characteristics presents a challenging task for the aircraft designer and architect. The goal of this study is rather to provide trends and sensitivities of relevant trades than to provide point designs. In order to do so and to capture the relevant sensitivities, a new design methodology has been developed and implemented in the iterative, multidisciplinary aircraft sizing process which will be described in further detail in the following sections.

2. DESCRIPTION OF METHODOLOGY

The design methodology is described in the following sections.

2.1. Overall Aircraft Design Process

The overall aircraft design methodology consist of disciplinary Level 0 and Level 1 tools which are connected via the Common Parametric Aircraft Configuration Schema (CPACS) [4]. These workflows are set up with the help of the remote component environment (RCE) [5] which allows for a fast and flexible adaption and addition of required disciplines.
The level 0 loop mainly consists of the conceptual sizing tool openAD, also used and described in more detail in [6]. This tool also serves as a design synthesizer in the level 1 workflow. All the level one methodology is described in [7].

2.2. Additional Disciplines

To capture all relevant aspects of a hydrogen fueled aircraft, additional methodology is required which is described below.

2.2.1. Thermodynamic Tank Model

To assess the thermodynamic phenomena of the cryogenic tank and to evaluate geometry and structural related sensitivities, a physics-based model has been developed. It calculates the rate of heat which is entering the tank during the mission and the related mass flow of hydrogen which has to be discharged or added to the tank to maintain the pressure in the predefined limits. The design pressure level inside the tank is chosen to be 1.5 bar. By increasing the design pressure level, the density of liquid hydrogen is decreasing. Additionally, the structural mass of the tank is increasing due to the higher pressure difference and the evaporation temperature also increases. Moreover, it has to be prevented that the air is entering the tank which would cause a hazardous situation. This determines the lower limit of the design pressure. The 1.5 bar is the optimum pressure level of several investigations [8], [3], [9] which is why it is set as a constant input.
The geometric input parameters are shown in Figure 1.

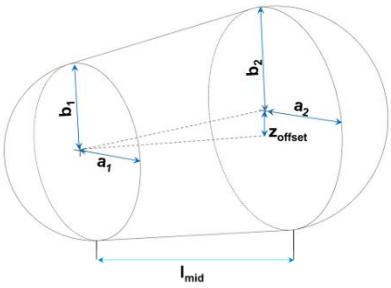

Figure 1. Geometric input parameters for the thermodynamic tank model

While the half axes of the two ellipse cross-sections a_1, a_2, b_1 and b_2 and the offset of the center and of the end sections are required inputs, the length of the tank is an optional input which can also be calculated by the maximum tank capacity. Additionally, the thermal related properties of the materials and the thickness of the different layers are needed which is displayed in Figure 2.
An additional input is the choice between an integral and a non-integral tank or a combination of both. It determines whether the outer wall is directly exposed by the outside air flow which has an influence on the heat management.
The heat fluxes which were considered are shown in Figure 3. These are the heat transfer from the outside to the gaseous phase and the liquid phase of the hydrogen, $\dot{Q}_{in,g}$ and $\dot{Q}_{in,l}$, the radiation from the outside to a defined part of the tank outer wall and from the inner tank wall which is covered by the gaseous phase to the liquid surface $\dot{Q}_{out,rad}$ and $\dot{Q}_{in,rad}$ and the heat transfer from the gaseous phase to the liquid phase $\dot{Q}_{gl}$.

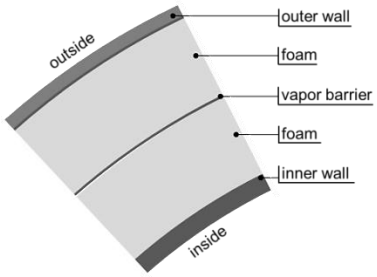

Figure 2. Wall layer of the thermodynamic tank model

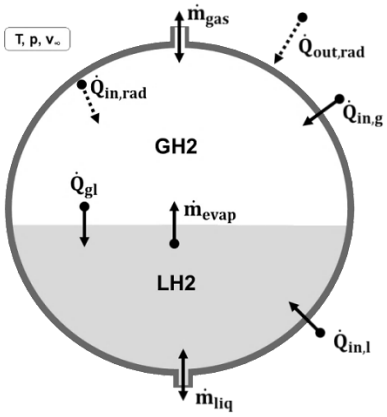

Figure 3. Thermodynamic tank model

For each point of the flown flight profile, the mass flow of the evaporated hydrogen is calculated dependent on the outside condition and the fill level of the tank. That means that for each time step, the transient heat fluxes are calculated which determines the current amount of boiled-off gaseous hydrogen also considering the current fuel flow which is needed for the required thrust at the recent flight condition. The fill level determines the Nusselt-number for the heat transition. For the gaseous part of the tank, the Nusselt-number is set to 17 which is determined by Brewer [9] who conducted a sophisticated study about that topic. For the liquid part of the tank, the surface is split up into three regions, similar as proposed by Winnefeld [3], because the heat transitions varies with the orientation of the wall in space. For the upper and the lower part of the tank inner wall, correlations from [10] are applied. The Nusselt-number of the side walls which are emerged in the liquid phase is calculated by Churchill and Chu [11], see equation (1). If the outside wall is exposed to the free airstream such as for integral tank architecture, a correlation according to [12] is applied. Otherwise, the method by Churchill and Chu [11] is used.

$$Nu = \left[0.852 + 0.387 \cdot Ra^{\frac{1}{6}} \Big/ \left(1 + (0.492/Pr)^{\frac{9}{16}}\right)^{\frac{8}{27}}\right]^2 \quad (1)$$

The heat dependency of the conductivity of the insulation material is extracted from [9].

The maximum tank volume is determined by the maximum required fuel mass together with additional 3% volume according to Brewer [9]. This rather optimistic 3% offset is needed to avoid the risk of over pressurizing the tank if it is filled to the maximum.

2.2.2. Additional Mass Calculation

2.2.2.1. Fuel Containment Mass

The mass of the fuel tank containment consists mainly of the four following parts.

- Inner structural wall
- Thermal isolation
- Vapor barrier
- Outer wall / fairing

The mass of the isolation is calculated by the volume and the density of the material. The volume is determined by the geometric tank model. The outer wall has the main function of containing the tank against foreign object damages. It is constructed by a Kevlar epoxy composite with a thickness of 1.57cm and a specific mass of 830.6kg/m^3, extracted from [9]. The vapor barrier has a thickness of 0.5cm and a specific mass of 0.22kg/m^2 [9].

Inner tank wall sizing

The required wall thickness of the pressure vessel can be computed by relating the circumferential stress to the yield strength of the material used. To compute the circumferential stress at the half-axes of an elliptic cross-section σ_a and σ_b, Dubbel [12] gives:

(2) $$\sigma_a = p \cdot \frac{a}{t} + c_1 \cdot p \cdot \left(\frac{a}{t}\right)^2,$$

(3) $$\sigma_b = p \cdot \frac{b}{t} + c_2 \cdot p \cdot \left(\frac{a}{t}\right)^2.$$

Here, a and b are the half-axes, p is the difference in pressure, t is the shell thickness and c_i are empirical coefficients depending on a/b. The relationships are a generalization of Barlow's formula, as both c_i turn to zero for $a/b = 1$.

Formulas (2) and (3) are validated using finite element analysis on shell models as shown in Figure 4. A unit mean radius of and a wall thickness of 0.01 are assumed.

The resulting stresses at the half-axis points are given in Figure 5 and compared to the results for the analytical functions. Both the analytical formula and the FEM analysis show a significant increase in circumferential stress when deviating from a circular cross-section, as illustrated by Figure 6. Furthermore, it is shown, that the analytical solution and the FEM solutions are in good agreement.

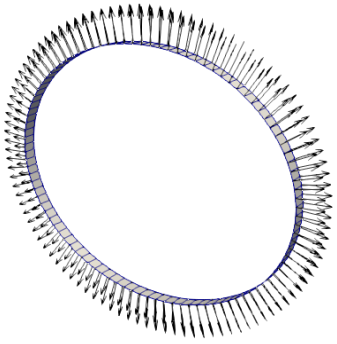

Figure 4: Finite element analysis model

Assuming that $a < b$, it also shows that σ_b is always the sizing parameter. Hence the required wall thickness can be determined by solving formula (3) for t.

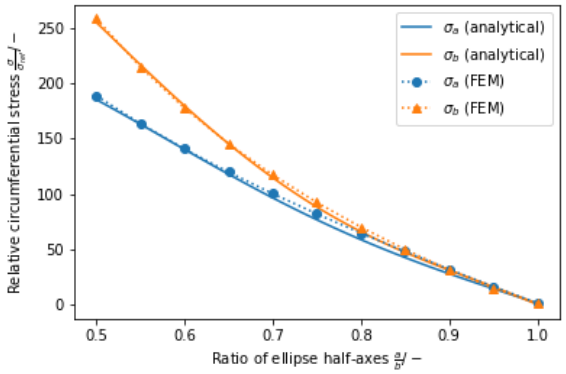

Figure 5: Comparison of analytical function to FEM results

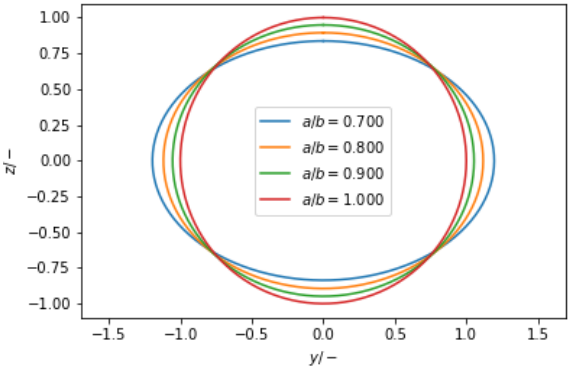

Figure 6: Cross-sections for different half-axis ratios

2.2.2.2. Fuel System Mass

Due to the more complex tank and the difference compared to conventional kerosene storing tanks, the system mass differs significantly. This is why the established empirical methods for conventional aircraft cannot be applied. Instead, the fuel system mass has been decomposed into subsystem masses which were estimated with correlation extracted from the literature [9] [13]. These subsystems are listed below:

- Boost pumps
- High-pressure pumps
- Engine fuel delivery lines
- Fuel transfer lines
- Gas out and drainage lines
- Engine fuel control system
- Fueling and defueling
- Tank vent and pressurization
- Splash back

The hydrogen is transferred in its liquid state and is gasified near the engine before injected into the combustion chamber. This is to assure a constant and finely adjustable fuel flow.

To determine the total mass of the fuel system, each of these subsystems is decomposed in its specific parts. Additionally, redundancy requirements are considered. This approach leads to a reliable fuel system mass estimation at conceptual level.

2.2.2.3. Additional Structural Mass

The integration of large cryogenic fuel tanks has impacts on the structure which is described below.
In case the cryogenic hydrogen is stored in external, wing mounted tanks, a pylon mass estimation is needed. Because the usual empirical based methods for pylon masses of turbofan engines are not valid due to their different dimensioning forces and loads, a new method is needed. This is why a correlation was extracted from data of the Lockheed C-130 Hercules with external fuel tanks [14] [15]. That leads to 0.014 pylon mass per total tank mass plus maximum fuel mass in the tank and systems. Because the external tanks of the C-130 are in a similar range considering the mass, this correlation can be applied at a conceptual level.
For the integration of the fuel tank on top of the fuselage, the effect on the structure has to be taken into account. The fuselage has to transmit the loads to the wing during flight and to the landing gear on the ground, which is especially challenging during touch down and crash occurrences. This effect has been considered by extracting a correlation from fuselage structural mass methods in the literature [16] [17] together with internal knowledge by using the difference of fuselage mass due to the wing, landing gear and engine position.

3. REFERENCE CONFIGURATION

3.1. Reference

The reference aircraft is an Airbus A320neo similar aircraft. It serves as a calibration and validation of the aircraft design methodology. The top level aircraft requirements (TLARs) are shown in the following Table 1.

Parameter	***Value***	***Unit***
Design Range	3100	nm
Cruise Mach-number	0.78	-
Take-off field length (SL ISA+15K)	2200	m
Landing field length (SL ISA+0K)	1850	m
Rate of climb capability	300	ft/min
ICAO Aerodrome Reference Code	Code C	-
Maximum payload	20000	kg
Design payload	17000	kg
Design cargo mass	2150	kg
Maximum cargo mass	5150	kg
Alternate distance	200	nm
Loiter time	30	min
Contingency	3%	-
PAX (design, 2 class)	165	-
Mass per PAX (design)	90	kg
Approach speed (with MLM)	131.5	kt (CAS)
Wing span limit	36	m

Table 1. Top Level Aircraft Requirements

The high-lift system is a single slotted fowler flap at the trailing edge and slats at the leading edge. All technology assumptions are based on the current A320neo. That means that the main parts of the fuselage as well as the wing are made of aluminum alloys and the engine has a bypass ratio of 12.5.

3.2. Baseline

In order to compare the hydrogen fueled tank integration concepts, a baseline aircraft which represents the best conventional configuration at the same entry into service (EIS) of 2045 is designed. To evaluate every influence of each step, several aircraft are investigated.
The technology assumptions which are valid for all baseline aircraft are displayed in Table 2 below and subsequently described and justified.

Technology Factor	***Value***
Fuselage structural mass	0.85
Wing structural mass	0.8 – 0.85
Furnishing	0.9
Engine performance	0.85

Table 2. Overview of applied technology assumptions

For the fuselage structural mass, a technology factor of 0.85 is assumed. This value can either be achieved by the application of CFRP (carbon fiber reinforced polymer) or GLARE (glass-reinforced aluminum laminate). Niemann et al. [18] investigated the potential of CFRP in the scope of the EU FP7 project “Advanced Lattice Structures for Composite Airframes” (ALaSCA) who state a mass saving potential of -14.3% compared to a conventional semi-monocoque concept with CFRP stiffeners. The potential of GLARE ranges between -12% to -30% for single aisle fuselage mass reduction according to [19] [20] [21].Both materials are already applied in the industry for example at the Airbus A350 and A380. A mass saving of -4% can be achieved with new aluminum alloys [22].
The wing structure is assumed to be constructed with CFRP. The mass saving compared to aluminum is calculated by the integrated methodology [23]. The exact difference cannot be deduced due to the changes in geometry and maximum wing loading. Nevertheless, the isolated potential of CFRP is expected to lie between -15% to -20%.
There is no further mass reduction assumed for the vertical tail-plane (VTP), the horizontal tail-plane (HTP), the pylons and the nacelles, because they are already mainly made of CFRP.
The last mass chapter which is changed is the furnishing mass. This contains amongst others the insulation, the crew seats and fixed crew rests, doors, toilets, hatracks, bins and floor covering. The technology factor applied is 0.9 due to new materials such as aerogels and multifunctional integration by new manufacturing methods. These 10% together with the assumed 0% mass saving for the design operating items which consist amongst other of the passenger seats, seem to be quite conservative considering the high mass saving potential of the interior. Nevertheless, the driving factors especially for this aircraft class will be manufacturability, cost, assembly but also recyclability or the higher demands of passengers regarding comfort and entertainment which will mitigate possible mass saving potentials.
The performance of the two geared turbofan engines is assumed to be 15% better than for the reference engine due to higher component efficiencies resulting in a higher optimum bypass-ratio (BPR), an increased overall

pressure ratio (OPR) and turbine entry temperature (T4). Additionally, new materials such as fiber reinforced ceramics reduce the need of cooling air leading to an increased efficiency. The mass penalty due to the increased OPR which basically means more stages and the increased BPR is not huge due to new materials such as fiber reinforced ceramics for some parts of the turbine or CFRP for the Fan which again has secondary effects on the whole engine mass.
In total, four baseline aircraft are designed which all have the same technology assumptions as described above. The first step is the Baseline 1 where the aspect ratio of the wing is kept constant.

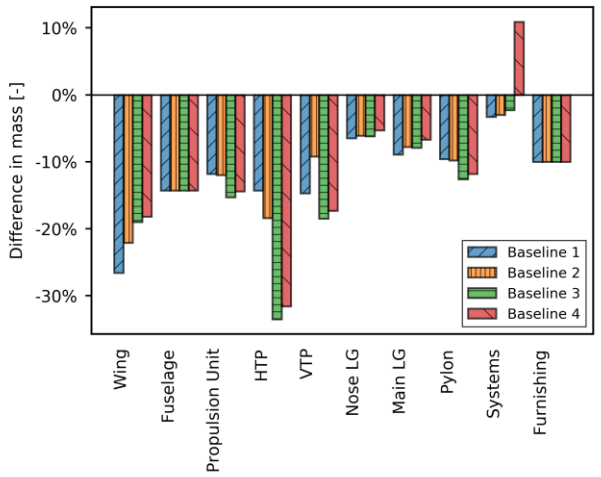

Figure 7. Change in mass of the baseline configurations relative to the reference aircraft

The relative changes in mass of the baseline concepts with respect to the reference aircraft are shown in Figure 7.
In order to better understand the phenomena leading to the results, a so called ladder chart is displayed in Figure 9. The major effect of the first step from the reference to the Baseline 1 is the improved engine efficiency whereas the mass effect due to new materials is with almost 8% also significant. The two rather small negative effects result from the increased engine mass and the higher wetted area of the nacelles mainly caused by the increased bypass ratio but also slightly mitigated by the reduced thrust requirements. The next step from Baseline 1 to Baseline 2 consists of a constant span of 36m which causes the aspect ratio to change. In this case, the aspect ratio increases because of the decreased mass of the aircraft leading to a reduced lift induced drag. In other words, less lift per span has to be produced. Nevertheless, this also results in an increase wing mass. The next step from Baseline 2 to Baseline 3 is the implementation of an advanced high-lift system, namely the change from a single slotted fowler flap to a double slotted one as it is applied at the Airbus A321. This results in a smaller wing due to the higher low speed performance which leads to an increased aspect ratio as well as a reduced wetted area and hence less drag. On the other hand, the system mass, mainly the hydraulic devices together with the structural mass of the wing and flaps increase. Because of the very small wing, there is not enough tank volume to achieve the same payload range characteristics as the other baseline aircraft. This is why an additional center tank (ACT) has to be installed which increases the tank volume but also the system mass, mainly the tank mass itself. Nevertheless, the Baseline 4 achieves the highest block-fuel saving potential of -24.4% which is why this is chosen to be the one to compare the hydrogen concepts in terms of block-energy with. General data of the reference and the baseline 4 are shown in the following Table 3.

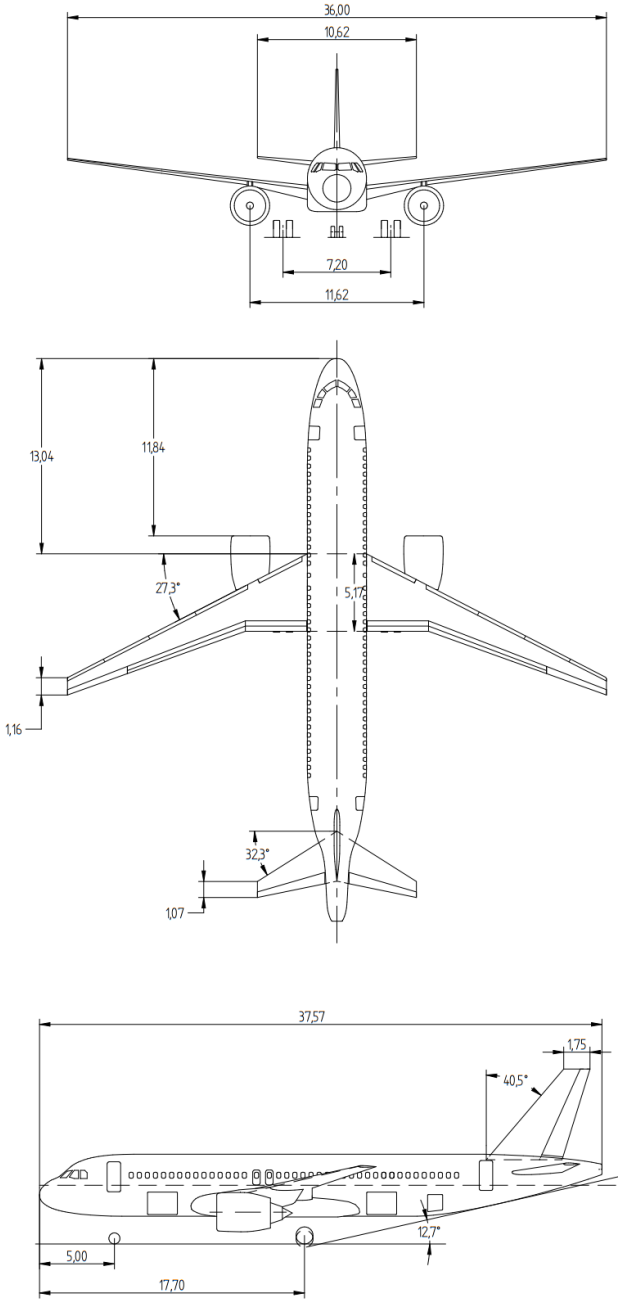

Figure 8. Three-side view of the baseline 4 with dimensions in meter

One issue which results from the high aspect ratio of the Baseline 4 of 12.4 is the landing gear integration which can be seen in Figure 8. Because the root section of the wing is further in front end the root chord is decreasing compared to the most rear center of gravity, the installation between the rear and the auxiliary spar is challenging or even not possible. This could lead to the integration of the landing gear into the fuselage which could be feasible without significant mass penalties.

Nevertheless, due to the changing aspect ratios throughout the conducted trades and to avoid disruptive occurrences, it is assumed that the landing gear is always installed at the wing.

Parameter	*Reference*	*Baseline 4*	*Unit*
MTOM	79016	70276	kg
OEM	44294	39838	kg
MZFM	64294	59838	kg
MLM	67400	62040	kg
Design block-energy	657.9	498.2	GJ
Thrust to weight	0.311	0.288	-
Wing loading (TO)	635.2	674.2	kg/m^2
Aspect ratio	10.3	12.4	-
Span	36	36	m

Table 3. General data of the Reference and the Baseline 4

3.3. Design Philosophy

It is important to describe the design philosophy in order to understand the effects leading to the results which are represented in section 4.
Whereas the passenger and the cargo compartment capacity are kept constant, the wing, the empennage, the engines and the landing gear geometry are highly flexible. The wing changes its longitudinal position depending on the most aft total center of gravity. That means a minimum static margin in flight is kept constant throughout the whole study. Because of a constant span limit of 36m, the aspect ratio changes with a changing reference wing area and maximum landing mass (MLM).

Usually, the ratio of the maximum landing mass to the maximum take-off mass is an input parameter. Nevertheless, if the variation in maximum take-off mass and operating empty mass is big and the same low speed performance has to be achieved, as it is the case for this study, this is not applicable anymore. If for example the aerodynamic efficiency or the thrust specific energy consumption is increasing whereas the structural mass is approximately the same, it is very likely to cut off a part of the full payload range characteristic. This is because the MLM is lower than the maximum zero fuel mass (MZFM) plus the reserve fuel mass at the most critical case of maximum range with maximum payload. In other words: It is not possible to land during this mission without using the reserve fuel and stay below the MLM. This is why a ratio of the block fuel for this specific mission is set as an input which leads to the MLM and ensures approximately the same total aircraft efficiency related margin between the MLM and the MZFM plus the reserve fuel.
The wing loading with respect to the maximum landing mass is an input parameter. With respect to the performance of the high lift system, this value ensures the same calibrated approach speed of 131.5kt for each aircraft. With this, the wing reference area and consequently the wing loading with the MTOM are iteratively calculated.
Whereas the reference area is determined by the approach speed, the thrust loading is calculated to achieve the required TOFL. That means that in this study, a rubber engine approach is applied which not just has an influence on the engine performance but also on the mass as well as the geometry and hence the nacelle drag.
The initial cruise altitude is not set as a requirement. It is optimized for each study and mission dependent on a combined aerodynamic-engine performance characteristic

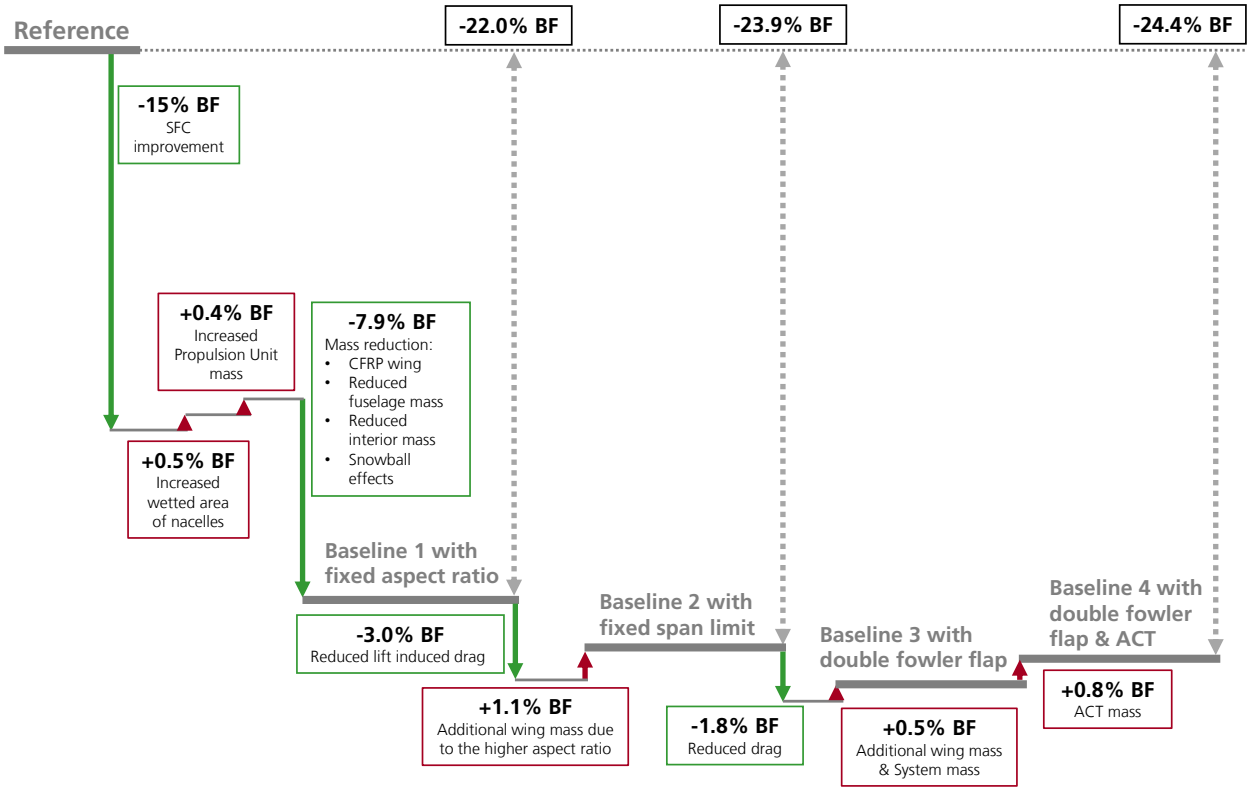

Figure 9. Ladder chart of the baseline configurations

as well for the hydrogen driven concepts on the tank behavior.
One additional important assumption is that with every concept, at least the market of the baseline aircraft has to be covered which means that the payload range characteristic has to be maintained.
It is possible to design an aircraft which is optimized for the assumed design mission. However, when it comes to the comparison between kerosene and a hydrogen fueled aircraft, the latter one would have a significant reduced operating ranges and payloads. This results from the fact that the aircraft loses much less mass during flight due to the higher gravimetric energy density of hydrogen. That means that the second section in a payload-range diagram which starts from the maximum range with maximum payload and ends if the maximum fuel capacity is reached, has a strongly reduced slope.
This can also be observed in Figure 10 where the two different design points for kerosene and hydrogen aircraft are displayed. The hydrogen one has been chosen in order to capture approximately the same payload range characteristic as for the Baseline 4 which is why it is at slightly higher range and payload. The comparison of the aircraft's efficiency is conducted at the design point of the kerosene fueled baseline 4.

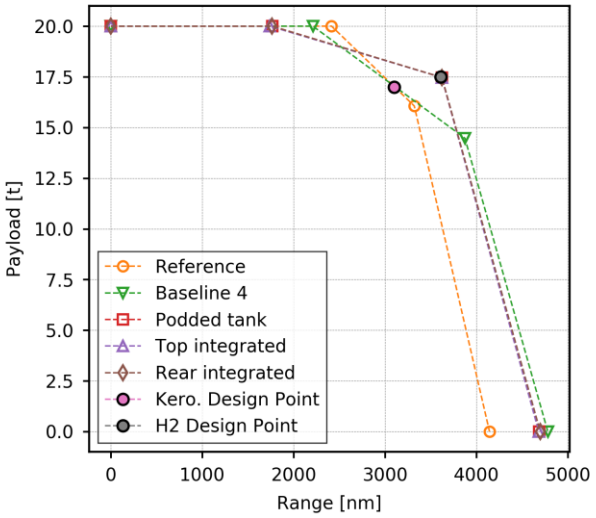

Figure 10. Payload-range diagram for the Reference, the Baseline 4 with one additional center tank and double slotted flaps, and the three hydrogen fueled concepts.

4. RESULTS

4.1. Tank Architecture and Material Selection

The major design decision concerning the hydrogen tank which has to be made is the applied tank architecture in terms of thermal isolation, load carrying material and whether or not to use an integral or non-integral structure. This is content of the subsequent three sections.

4.1.1. Total Tank Wall Composition

General speaking there are two ways of how to order the tank structure, namely an integral and a non-integral one. While for an integral tank architecture the inner wall acts also as the load carrying part, for a non-integral variant, the tank is located inside an outside structure such as a fuselage. The fact that the tank has to be inspected several times during its lifetime results in the major difference between these two architectures. For a non-integral version that would entail the application of a removable tank which is highly impractical for tank shapes which should be as big and as spherical as possible, described in section 4. For integral architectures, the insulation can be inspected from the outside which makes the inspection much easier and lowers the structural mass penalties.
The question of which architecture to use is relevant if the tank is integrated inside the fuselage or somewhere else in the aircraft's structure. For the podded version with the tanks under the wing it is obvious that just an integral concept is reasonable.

4.1.2. Isolation Methods and Material

In order to avoid the cryogenic hydrogen to boil off, cooling is necessary. The major requirements are a lightweight characteristic, very low thermal conductivity, similar thermal expansion coefficients and a high standard of safety. Additionally, production and maintenance cost as well as the technical readiness level (TRL) of the architecture are of major importance. There are several methods described in the literature [9] [24] which are listed below.

- Foams
- Aerogels
- Vacuum
- Multi-Layer Insulation (MLI)

It is not in the scope of this publication to describe the differences between these architecture in detail which is why only a very brief description and explanation of why closed cell foams have been applied is provided.
While the vacuum and the MLI architecture have very low thermal conductivities, they need vacuum which leads to a heavy tank wall and increased system mass. Furthermore, the loss of vacuum represents a serious risk [24]. Despite the low thermal conductivity of aerogels, the limited mechanical properties together with the high risk of this new material leads to the forth architecture. Closed cell foam is used mainly due to its lightweight and low cost characteristics. More precisely, foam with a density of 35 kg/m^3 and a thermal conductivity of between 0.0035 W/m/K and 0.03 W/m/K dependent on the temperature extracted from Brewer [9] is applied.

4.1.3. Inner Wall Material

The inner wall of the liquid hydrogen fuel tank carries the loads, especially caused by the difference in pressure which can reach up to 2bar at high altitudes.
Additional to the mechanical loads and hence the lightweight aspect, the material has to sustain cryogenic temperatures without embittering, it has to avoid massive permeation of hydrogen through the tank wall and the thermal expansion coefficient has to fit to the other materials used.
Mital et al [24] showed, that CFRP is the most mass efficient material. Nevertheless, the production costs are most probably higher than for well-known aluminum alloys. Still, because the future cost for operators will be most likely more energy consumption sensitive, a CFRP inner wall material is chosen.
The European Union funded project CHATT (Cryogenic Hypersonic Advanced Tank Technologies) which had the objective to investigate CFRP cryogenic hydrogen tanks proved at least 30% mass saving compared to aluminum

and stated a technical readiness level (TRL) of 3-4 in 2015 [25].
A safety factor of 2 has been applied which has also been used by Brewer [9]. This is a rather conservative approach to cope with the insecurities at this stage of the study.

4.2. System Safety Concept

Besides the containment of the tank itself, the feed lines have to be considered in terms of safety aspects. Generally speaking, it has to be avoided that hydrogen is entering the cabin which would result in a hazardous situation. For the podded version, this is not a big issue despite the cross feed line from one tank to the engine on the other side of the fuselage, in case this is required. Nevertheless, the part of this line which is crossing the fuselage is quite small which means that either special containers or vented compartments could be applied or the lines could be placed at the outside of the fuselage.
For the rear integrated version, the feed lines could also be placed at the outer skin of the fuselage. Additionally, in this configuration it has to be avoided that the fuel is entering the cabin through the rear bulkhead. The flying testbed from Tupolev, the Tu-155 solved this issue by pressurizing the space between the cabin and the rear tank [26]. The integration of the fuel tanks on top of the fuselage is not that critical than the rear integration due to the ascending characteristic of gaseous hydrogen. Nevertheless, despite several subjects which need to be clarified by further test, the cryoplane project concluded a similar safety level than for kerosene driven aircraft [27].

4.3. First Downselection

The first step was a collection of all possible positions and concepts of where to store the voluminously hydrogen in an aircraft.
Generally, it is possible to place the LH2 tanks above, below or beside the fuselage, behind, in front or behind and in-front the cabin and in pods under and above the wing. Inside the wing has been excluded due to the lack of available volume. The placement below the cabin inside the cargo compartment, below and beside the fuselage has also been excluded mainly due to safety reasons.
The need of a door between the cockpit and the cabin is not fully answered yet which leads, together with the negative structural mass effects, to the exclusion of the placement between cockpit and cabin. Remaining concepts are behind the cabin, above the fuselage and in pods at the wing. The placement above the wing could lead to a neutral aerodynamic performance especially in transonic flight regimes. Nevertheless, this is still under investigation which is why the pods were installed below the wing. These three variants have been investigated und the results are described in the next sections.

4.4. Thrust to Weight Trade

Because of the high gravimetric density of hydrogen, the aircraft mass is reduced significantly. Generally speaking, the main effect is the fuel mass itself. This means, that the ratio between MTOM and MLM is higher than for kerosene driven aircraft, following the assumptions described in section 3.2. This results in a reduced wing loading which slightly mitigates the mass reduction.
Another consequence of the strongly reduced fuel mass is that the top of climb (TOC) condition is more challenging because of the difference in aircraft mass between take-off and TOC is much less than for the baseline aircraft. This leads to a specific study to optimize the thrust to weight ratio. Basically, this is a trade between more mass and wetted area of the engines against a more suitable cruise altitude to operate the aircraft near the maximum aerodynamic performance. Changing the wing loading would not help, because it is determined by the approach speed and therefor can just be reduced to avoid a violation of that.

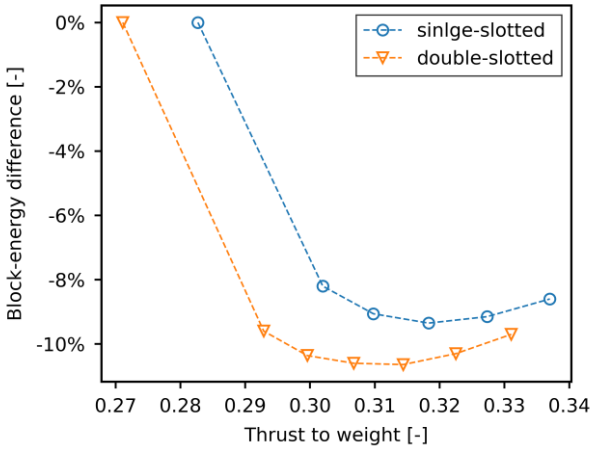

Figure 11. Thrust to weight trade for hydrogen fueled aircraft with single and double slotted flaps

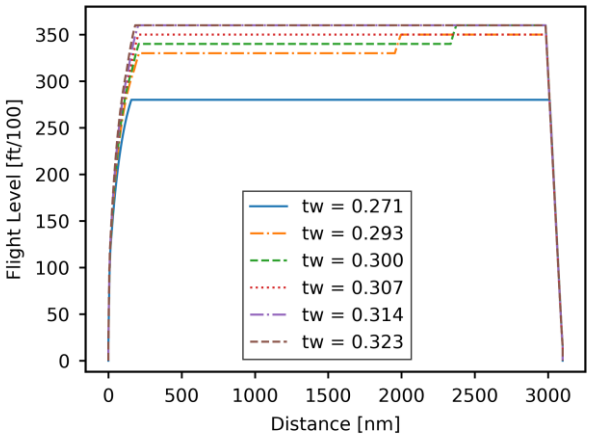

Figure 12. Vertical flight profiles for different thrust to weight assumptions

A decreased wing loading would have the opposite effect; hence the optimum cruise altitude would even increase. One additional possible trade would be a different high lift system as conducted here. In Figure 11, the difference in block-energy of different thrust to weight conditions for two high lift systems is displayed. It can be observed that up to a certain thrust to weight ratio, the energy consumptions decreases dramatically. At the right hand side, the additional mass of the engine and the drag of the nacelles overweight the advantages of the increased cruise altitude or the optimum altitude is already reached without the need of more thrust. This can also be seen in Figure 12 where the vertical flight profile is displayed. It can be observed, that especially the first change in altitude is huge whereas the steps become smaller at higher thrust to weight assumptions. For the last to ratios, the altitude is even the same which indicates that the optimum altitude

has been reached.
Additionally, it can be seen that the optimum of the aircraft with the double slotted fowler flaps is more at lower thrust to weight ratios which is a result from the reduced wing and hence increased wing loading in mid cruise. That leads to a lower optimum altitude to fly near the maximum lift to drag ratio resulting in a reduced required thrust to reach that altitude.
This is meant to be a preparatory study to get a range of the possible thrust to weight ratios. The results also show the enormous difference in block energy if this problem would not have been considered.

4.5. Rear integrated Tanks

The first concept which has been investigated is the integration of the hydrogen tank at the rear. Two tanks are located behind the rear bulkhead of the cabin which can be seen in Figure 13.

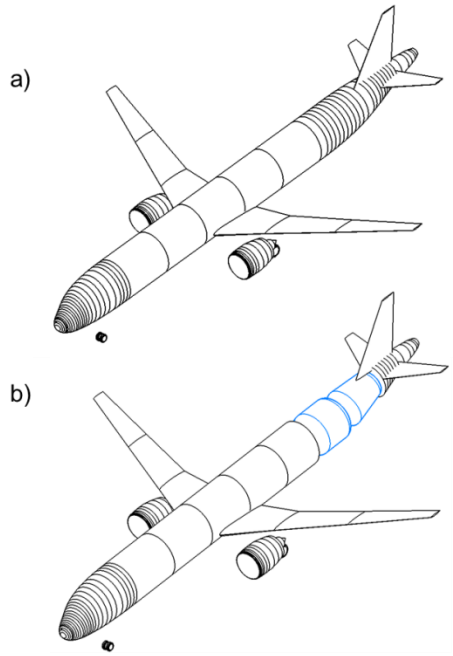

Figure 13. Geometry of rear integrated tank concept with the outer shape a) and the visualization of the two tanks b)

The outer dimensions in terms of width and height were extracted from the fuselage cross-section while the length and the inner dimensions are iteratively adapted dependent on the maximum fuel mass and the thickness of the total tank wall. The relative block-energy difference referred to the Baseline 4 which is the most efficient one in terms of block-energy over a variation of the insulation thickness is shown in Figure 14. The minimum difference occurs at an insulation thickness of 7 cm. This optimum is mainly determined by the characteristic behavior of the insulation mass and the amount of boil-off relative to the block energy. Figure 14 shows that with increased insulation thickness, the relative boil-off reduced due to the better isolation capabilities while the insulation mass increases.
Despite this specific trade, the main differences between this concept and the kerosene fueled Baseline 4 is the additional drag and structural mass due to the increased fuselage length of 45.7m. The fuselage mass increases by 28% and the lift to drag ratio at mid-cruise condition decreases by 5%. Additionally, the nose and main landing gear mass combined increase to assure the same rear clearance angle which leads together with the fuel containment and additional system mass to a 11% higher operational empty mass (OEM). Relevant results are also listed in Table 1 in section 5.

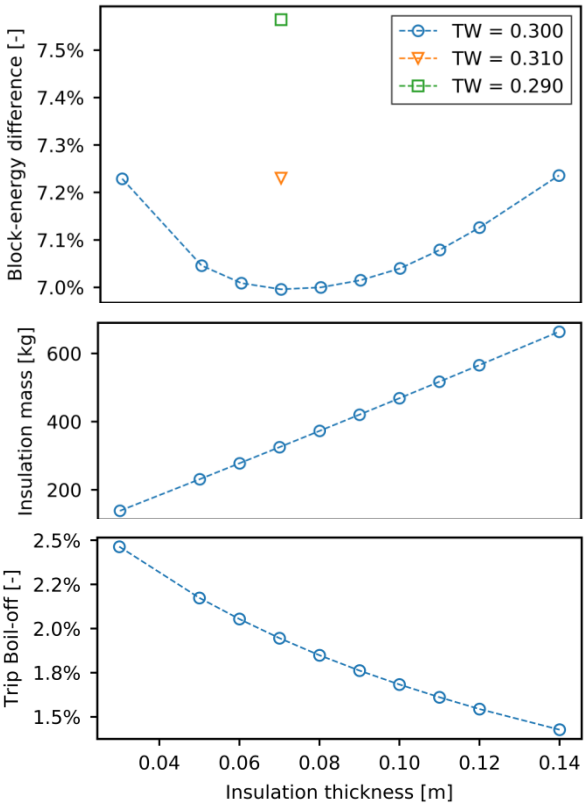

Figure 14. Results of the rear integrated tank concept

Furthermore, despite the preparatory study to get a range of possible optimum thrust to weight ratios, two further designs have been calculated to verify and exclude smaller variations. One with a thrust to weight ratio of 0.31 and one with 0.29 which both show higher design block energy consumptions.

4.6. Podded Tanks

The next tank position which has been investigated is the storage of liquid hydrogen under the wing. At the beginning of this study it was unclear if this is even possible considering the limited space and the expected strong increase in aerodynamic drag. The result is that it is feasible because of the already very efficient baseline. Nevertheless, installing the big pods below the wing without mitigating the high-lift performance and without violating the limits of the side clearance and rear clearance angles is a challenge.
The limiting side clearance angle is set to 5° with deflated struts and tires according to [28]. In particular it must be considered that the plane determined by the rear and the side clearance limit is not intersected by the tank structure. Before starting a trade of different tank radii, the optimum thrust to weight to reach the flight altitude where it is possible to fly at the optimum lift to drag ratio without violating the take-off requirements has been investigated. This can be seen in Figure 15 where the optimum lays

around 0.318.
Again, the big influence of the best thrust to weight ratio is noticeable. This ratio is applied to the subsequent trade study between the insulation thickness and the inner maximum radius of the hydrogen tanks and their effect at the block energy consumption compared with the kerosene fueled Baseline 4.

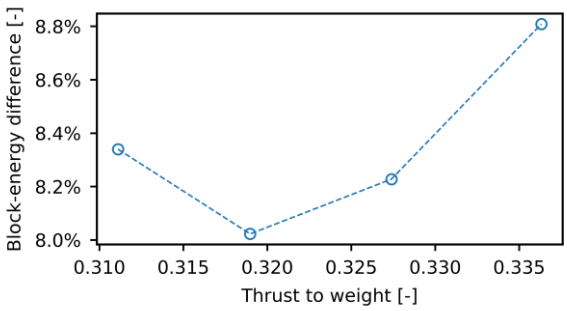

Figure 15. Thrust to weight trade of the podded tank version

It can be seen in Figure 17 that the bigger the radius, the lower the block fuel starting with 1.15m and going up to 1.55m where the theoretical limit of installation constraints is reached. It can also be observed that the gradient is decreasing with increasing radii. For the aircraft concept with 1.45m and 1.55m the landing gear length has to be increased in order to stay in line with the side clearance limits. An isometric view of this concept is shown in Figure 16.

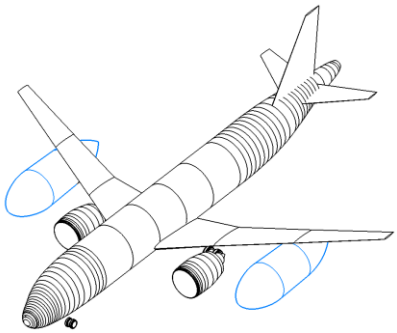

Figure 16. Geometry of top integrated tank concept

The trend which is shown in Figure 17 can be better described by looking at the behaviour of the tank and its aerodynamic performance. This is visualized in Figure 18 for a constant insulation thickness of 10cm. The fuel containment mass as well as the relative boil-off rate is decreasing with increasing maximum inner tank radius. This results from the reduced surface area per volume while approaching a circular tank shape. Nevertheless, the pressure drag part increases as well as the dead volume due to aerodynamic fairings. The increasingly challenging aerodynamic tank-wing interaction has not been considered which will probably shift the optimum to slightly smaller radii.
All in all, the feasibility of this architecture as well as the performance quantification is the major result of this study.

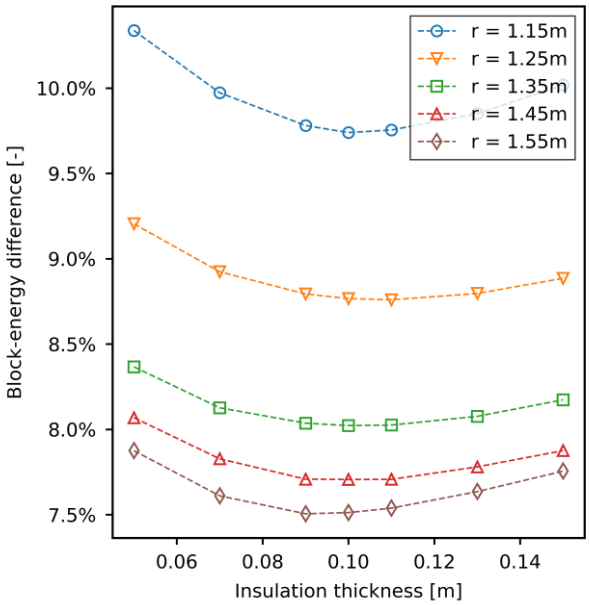

Figure 17. Results of the trade between different tank radii and the insulation thickness of the podded tank architecture

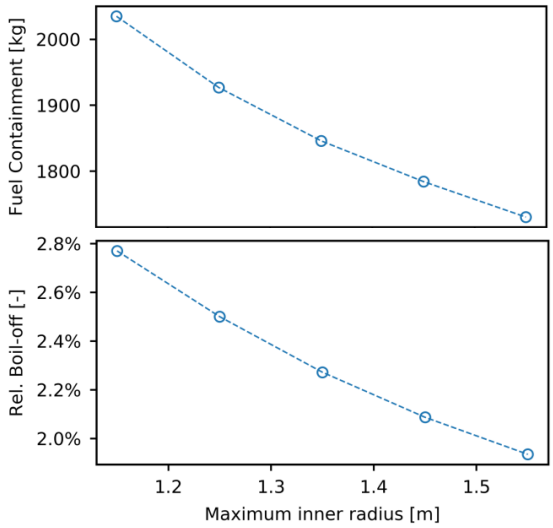

.

Figure 18. Fuel containment mass and relative boil-off dependent on different maximum inner tank radii

4.7. On top integrated Tanks

The last architecture which has been investigated is the integration of the liquid hydrogen tank on top of the fuselage which can be seen in Figure 19 below.
The trade between the insulation thickness and the maximum inner radius of the tanks and the effect at the block-energy consumption is shown in Figure 20. Two tanks are integrated which increase in diameter from 0.8m and 1.0m up to 1.2m or 1.4m for the two versions, while approaching approximately the center of the fuselage length and vice versa.

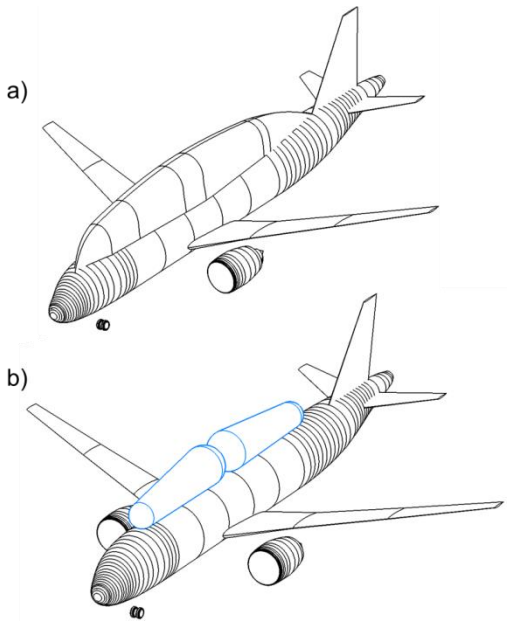

Figure 19. Geometry of top integrated tank concept with the outer shape a) and the visualization of the two tanks b)

It can be observed, that the small change in maximum radius from 1.4m to 1.2m results in a significant performance difference of almost 2.5% block-energy. While about 1% is directly coming from the increased boil-off due to the rather small and thin tanks, the additional fuel containment mass and fairings as well as snowball effects do the rest.
Nevertheless, this concept is the most efficient one in terms of design block-energy difference compared to the rear and podded hydrogen versions.

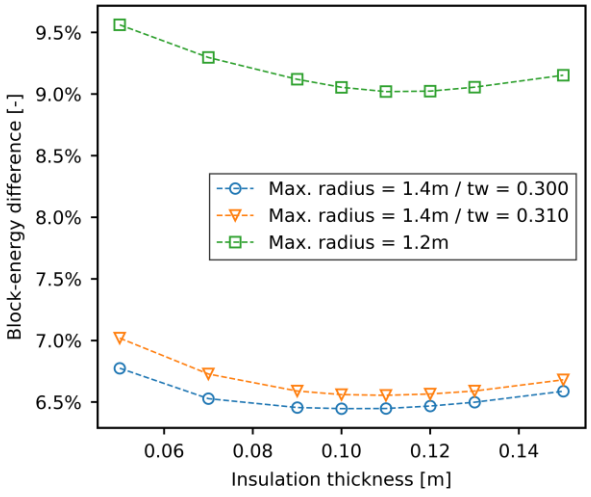

Figure 20. Results of the trade between different tank radii and the insulation thickness of the podded tank architecture

5. SUMMARY AND CONCLUSION

Three liquid hydrogen tank integration concepts have been investigated at the timeframe of EIS of 2045, one with the tanks at the rear of the fuselage behind the cabin, one on top of the fuselage and one with pods under the wing. All three showed, that they are feasible with block-energy drawbacks below 8% compared to the best kerosene fueled baseline with a double slotted fowler flap, increased engine efficiency, CFRP wing and an additional center tank (ACT).
Table 4 summarizes relevant results of the three concepts.

Parameter	***Rear***	***Top***	***Pod***	***Unit***
MTOM	67819	66045	64584	kg
OEM	44334	42605	41084	kg
MZFM	64334	62605	61084	kg
MLM	65069	63331	61823	kg
Design block-energy	533.0	530.3	535.6	GJ
Thrust to weight	0.300	0.310	0.319	-
Wing loading (TO)	620.4	620.7	621.8	kg/m^2
Aspect ratio	11.9	12.2	12.5	-
Insulation thickness	7	10	9	cm
Fuel system mass	781	627	630	kg
Fuel containment mass*	1651	2429	2190	kg
Rel. trip boil-off	1.9	2.5	2.0	%

*including the additional masses such as support structure, safety features or pylons

Table 4. Resuts of the three hydrogen cncepts with the optimum insulation thickness

It can be observed that the maximum take-off mass (MTOM) of all three concepts is higher than the baseline, see Table 3, while the operational mass empty is lower. Despite the decreased MTOM the maximum landing mass (MLM) increases for the rear and top integrated version because the fuel mass decreases dramatically which moves the MTOM closer to the MLM. This phenomenon reflects also the decreased wing loading at take-off condition compared to the baseline because the same low speed approach performance is required while the ratio between MLM and MTOM is decreasing. The thrust to weight ratio is higher for the hydrogen fueled aircraft. That does not result from the take-off field length (TOFL) or one engine inoperative (OEI) requirements but from the necessity to reach altitudes where the flight condition allows flying at the maximum aerodynamic performance. That means that the maximum thrust is driven by the aircraft's efficiency rather than take-off or OEI cases. The explanation of that is first, the MTOM is reduced, second, during the climb segment, the hydrogen fueled concepts lose much less mass than kerosene fueled aircraft and third, the thrust which is required to achieve the same take-off performance decreases which makes it challenging to have enough thrust at cruise altitude. Additionally, the altitude for optimum aerodynamic performance increases which makes it even more challenging for the engines, because the wing loading at mid-cruise is lower than for the baseline.
For all three concepts, trade studies have been conducted to find the optimum insulation thickness. While for the rear version, the insulation thickness with the minimum energy consumption has been determined to be 7cm, the result for the podded version is 9cm and for the version on top 10cm. These different thicknesses can be explained with the possible tank shapes. For the rear concept, two almost circular tanks could be installed which requires less insulation material to achieve the same boil-off rate. For

the top version, the tanks are rather long which results in thicker insulations.
The boil-off correlates with the three different insulation thicknesses.
The main effects which drive the overall aircraft efficiency are displayed in Figure 21 together with the total design block-energy difference compared to the baseline aircraft.
The averaged positive effect of the reduced mass during the flight segment is very strong for the podded version while it is almost neglect able for the rear integrated tanks. This shows the structural benefit of the podded version compared to the rather heavy aircraft with a very long fuselage.

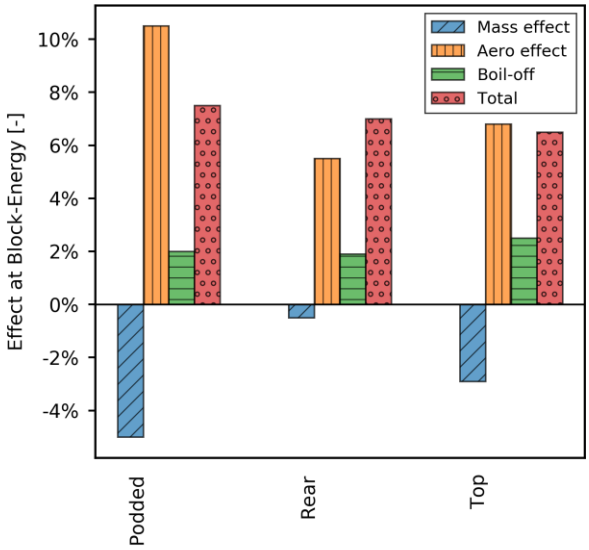

Figure 21. Vizualization of major effects at the block-energy compared witht the Baseline 4

The aerodynamic drawback is worst for the podded variant with an averaged lift to drag decrease of more than 10% while the rear tank concept is aerodynamically the most efficient. The third strong effect is the boil-off which however is lower than the previous two.
Nevertheless, this boiled-off hydrogen can be further used or stored with an additional pressure tank which will again cost mass and energy. This requires a sophisticated investigation which is out of the scope of the current study.
Subsequently, general advantages, disadvantages and characteristics for the three concepts are described.
The podded version has the lowest structural mass while the worst aerodynamic and overall performance because the additional area is completely exposed to the outside flow. Nevertheless, the increase safety due to the separation of the fuel and the fuel system from the cabin on the one hand and the possibility of dropping the tanks while an emergency landing similar to the engine which fall off if they get the wrong loads on the other hand. Additionally the fuel tanks can be accessed very well which decreases the effort for operations and maintenance.
One open question is the disc burst occasion. If the tank has to be located outside the burst cone, it is not possible anymore to cope with the rear clearance angle and especially with the combination of rear and side clearance angle.
This disc burst problem is not an issue for the concept with the tanks at the rear. For the top integrated version, this could also be avoided but would lead to additional dead volume and hence wetted area.
An further general finding of this study is that the snowball effects are much more sensitive regarding changes in efficiency and mass than for kerosene aircraft due to the strong influence on the fuel containment mass and the wetted area.
Finally, all three concepts are feasible and show comparable design block-energy consumptions with small variations of maximum 1.0% between their optimum. Compared to the kerosene baseline, the block-energy consumptions increase between 6.5% and 7.5%. Still this is not a big difference considering the efficiency variations in the hydrogen and synthetic kerosene production chain and the further optimization potential described in the subsequent section.

6. OUTLOOK

Further investigations resulting from this study could be a multidisciplinary study of how to use or store the boiled off gaseous hydrogen to minimize this loss term. The engine performance should also be investigated in further detail because in spite of the low mass flow, the huge temperature difference could be used to increase its efficiency. These two aspects would result in a reduced drawback compared to the kerosene baseline.
Additionally, instead of starting with an Airbus A320neo similar aircraft, a new design with an adapted cabin layout and fuselage dimensions could result in further benefits.
Last but not least, the implementation of the aircraft level performance into a wider assessment range based on a system of systems approach will be shown in future work. This would mainly include the production efficiencies of power to liquid (PtL) and hydrogen generation as well as the comparison of the climate impact and its dependencies of altitude and Mach-number and the NOx emissions around the airport within the landing and take-off cycle (LTO).

ACKNOWLEDGMENTS

The authors would like to thank Björn Nagel, Erik Prenzel, Sebastian Wöhler and Johannes Hartmann for their interest and support.

NOMENCLATURE

Abbreviations

ACT	Additional center tank
BE	Block energy
BF	Block fuel
BPR	Bypass ratio
CAS	Calibrated airspeed
CFRP	Carbon fiber reinforced polymer
CS2	Clean Sky 2
DLR	German Aerospace Center
EIS	Entry into Service
FEM	Finite Element Method
FL	Flight level
FPR	Fan pressure ratio
GH2	Gaseous hydrogen
HTP	Horizontal tail-plane
ICA	Initial cruise altitude
ICAO	International Civil Aviation Organization
ISA	International Standard Atmosphere
MBSE	Model based system engineering
MLM	Maximum landing mass
MTOM	Maximum take-off mass
MZFM	Maximum zero fuel mass
Nu	Nusselt number
OAD	Overall Aircraft Design
OEI	One engine inoperative
OEM	Operational empty mass
OPR	Overall pressure ratio
PAX	Passenger
Pr	Prandtl-number
PTL	Power to liquid
$\dot{Q}_{in,g}$	Heat transfer from outside to the gaseous phase
$\dot{Q}_{in,l}$	Heat transfer from outside to the liquid phase
$\dot{Q}_{out,rad}$	Radiation at outer wall
$\dot{Q}_{in,rad}$	Radiation from inner wall to liquid surface
$\dot{Q}_{gl}$	Heat transfer from the gaseous phase to the liquid phase
Ra	Rayleigh number
RCE	Remote component environment
SL	Sea level
T4	Turbine inlet temperature
TLAR	Top level aircraft requirements
TOC	Top of Climb
TOFL	Take-off field length
VTP	Vertical tail-plane

REFERENCES

[1] "European Commission, Flightpath 2050," Europe's Vision for Aviation, 2011.

[2] H. G. Klug, "CRYOPLANE, Hydrogen Fuelled Aircraft," Submission for the Energy Globe Award 2001, Category "Transport", Hamburg, 2000.

[3] C. Winnefeld, T. Kadyk, B. Bensmann, U. Krewer and R. Hanke-Rauschenbach, "Modelling and designing cryogenic hydrogen tanks for future aircraft applications," *Energies,* vol. 11, no. 1, p. 105, 2018.

[4] German Aerospace Center, Institute of System Architectures in Aeronautics, 2018. [Online]. Available: https://www.cpacs.de/. [Accessed 2019].

[5] D. Seider, M. Litz, M. Kunde, R. Mischke and P. & Kroll, "RCE: Distributed, Collaborative Problem Solving Environment," 2012.

[6] G. Atanasov, J. van Wensveen, F. Peter and T. Zill, "Electric Commuter Transport Concept enabled by Combustion Engine Range Extender," in *German Aerospace Congress*, Darmstadt, 2019.

[7] D. Silberhorn, C. Hollmann, M. Mennicken, F. Wolters, F. Eichner and M. Staggat, "Overall Design and Assessment of Aircraft concepts with Boundary Layer ingesting Engines," in *German Aerospace Congress*, Darmstadt, 2019.

[8] D. Verstraete, The Potential of Liquid Hydrogen, Cranfield University, 2009.

[9] G. D. Brewer, Hydrogen aircraft technology, New York: Routledge, 1991 .

[10] Wärmeatlas, V. D. I., Düsseldorf : VDI-Verlag, 1988.

[11] S. W. Churchill and H. H. Chu, "Correlating equations for laminar and turbulent free convection from a vertical plate," *International journal of heat and mass transfer ,* vol. 18, no. 11, pp. 1323-1329, 1975.

[12] K. H. Grote, J. Feldhusen and eds, DUBBEL: Taschenbuch für den Maschinenbau, Springer-Verlag, 2011.

[13] K. Thudt and J. Ehrhardt, Cryoplane Metallic Tank Design, 1994.

[14] Lockheed Martin Aeronautics Company, "Maintenance Instructions Fuel Systems," 1980.

[15] J. P. R. Policarpo, "Sealant Joints in Aircraft Integral Fuel Tanks," 2014.

[16] E. Torenbeek, "Synthesis of subsonic aircraft design," Springer, Delft, 1982.

[17] F. Dorbath, "Large Civil Jet Transport (MTOM > 40t), Statistical Mass Estimation," Luftfahrttechnisches Handbuch (LTH), 2013.

[18] S. Niemann, B. Kolesnikov, H. Lohse-Busch, C. Hühne, O. M. Querin, V. V. Toropov and D. Liu, "The use of topology optimisation in the conceptual design of next generation lattice composite aircraft fuselage structures," *The Aeronautical Journal,* vol. 117, no. 1197, pp. 1139-1154, 2013.

[19] J. W. Gunnink, A. Vlot, T. J. De Vries and W. Van Der Hoeven, "Glare technology development 1997–2000," *Applied Composite Materials,* vol. 9, no. 4, pp. 201-219, 2002.

[20] R. C. Alderliesten, C. D. Rans, T. Beumler and R. Benedictus, "Recent Advancements in Thin-Walled

Hybrid Structural Technologies for Damage Tolerant Aircraft Fuselage Applications," *ICAF 2011 Structural Integrity: Influence of Efficiency and Green Imperatives,* Vols. Springer, Dordrecht, pp. 105-117, 2011.

[21] FOKKER Aerostructures, "Along the bond line, Groundbreaking aircraft structures".

[22] Aleris Corporation, "Aerospace Aluminum AA5028 AlMgSc, The Strong Lightweight," 2015.

[23] G. P. Chiozzotto, "Initial Weight Estimate of Advanced Transport Aircraft Concepts Considering Aeroelastic Effects," in *55th AIAA Aerospace Sciences Meeting*, 2017.

[24] S. K. Mital, J. Z. Gyekenyesi, S. M. Arnold, R. M. Sullivan, J. M. Manderscheid and P. L. Murthy, "Review of current state of the art and key design issues with potential solutions for liquid hydrogen cryogenic storage tank structures for aircraft applications," 2006.

[25] M. Sippel, A. Kopp, D. Mattsson, J. Freund, I. Tapeinos and S. Koussios, "Final Results of Advanced Cryo-Tanks Research Project CHATT," in *6th European Conference for Aeronautics and Space Sciences (EUCASS)*, 2015.

[26] *Soviet designer Tupolev describes hydrogen fuel safety measures,* Flight International, 18 February 1989.

[27] Airbus Deutschland GmbH, "Liquid Hydrogen Fuelled Aircraft – System Analysis, Final Technical Report (Published Version)," 2003.

[28] J. Roskam, Airplane Design: Preliminary configuration design and integration of the propulsion system, DARcorporation, 1985.

[29] R. Becker, F. Wolters, M. Nauroz and T. Otten, "Development of a gas turbine performance code and its application to preliminary engine design," in *Deutscher Luft-und Raumfahrt Kongress* , Bremen, 2011.

[30] European Aviation Safety Agency, "Type-Certificate Data Sheet, No. IM.E.093 for PW1100G-JM Series Engines," 2019.

[31] K. Horstmann, "Ein Mehrfach-Traglinienverfahren und seine Verwendung für Entwurf und Nachrechnung nichtplanarer Fluegelanordnungen," DFVLR, Braunschweig, 1987.

[32] M. Iwanizki, M. J. Arzberger, M. Plohr, D. Silberhorn and T. Hecken, "Conceptual Design Studies of Short Range Aircraft Configurations with Hybrid Electric Propulsion," Dallas, Texas, 2019, (to be published).

[33] A. Westenberger, "Hydrogen fueled aircraft," *AIAA International Air and Space Symposium and Exposition: The Next 100 Years,* p. 2880, 2003.